2019 IEEE International Conference on Systems, Man and Cybernetics (SMC)
Bari, Italy. October 6-9, 2019

Automated Alzheimer's Disease Diagnosis using a Low-Density EEG Layout and New Features based on the Power of Modulation Spectral "Patches"

Raymundo Cassani and Tiago H. Falk
Institut National de la Recherche Scientifique (INRS-EMT),
University of Quebec, Montreal, QC, Canada

***Abstract*— Over the last decade, biomarkers to detect Alzheimer's disease (AD) have been proposed based on electroencephalography (EEG), in particular resting-state EEG (rsEEG). Typically, medium- or high-density research-grade EEG layouts with 16+ electrodes have been utilized and features extracted from traditional frequency subbands. As the quality of EEG sensors have gone up in recent years and low-density devices are emerging, it is not clear if accurate diagnosis can still be achieved with such solutions. Moreover, recent research has suggested that decomposing EEG into the five traditional frequency subbands may not be optimal for AD. In this paper, we describe a first attempt at developing an automated AD diagnostic system based on a low-density EEG layout (7 channels) directly from raw EEG signals. Such an approach would make the final solution "light", both in terms of cost and computational complexity. To achieve this goal, new features are required that are robust to artifacts present in the raw EEG. We present results with a cohort of 54 participants and show that AD diagnostic accuracy as high as 79.6% can be achieved with the proposed solution, thus in line with what can be achieved with a 20-channel layout and manual selection of artifact free EEG segments (81.5%). Further optimization is needed for other tasks, such as measuring AD severity level.**

I. Introduction

Alzheimers disease (AD) is a neurodegenerative terminal disorder that accounts for nearly 70% of of all dementia cases worldwide. Dementia global prevalence is projected to rise from 47 million in 2018 to 75 million cases by 2030, with most (over two thirds) of the affected individuals coming from low- and medium- income countries [1]. Nowadays, there is only palliative care to treat the symptoms of AD [2]. Although there is no cure for AD, early and accurate diagnosis could improve the quality-of-life of patients and their caregivers, as patients would preserve their independence for longer, thus preventing psychiatric related symptoms such as depression or psychosis. This can also lead to a reduction in personal and societal costs associated with AD. Moreover, it is likely that novel drugs to treat AD symptoms will be more efficient in early stages of the disease [3].

Current AD diagnosis is performed using patient's medical history and extensive mental status examinations following the criteria developed by National Institute on Aging and the Alzheimers Association (NIA-AA) [4]–[7]. These criteria consider the use of biomarkers derived from neuroimaging techniques (e.g. magnetic resonance imaging (MRI), computed tomography (CT) and positron emission tomography (PET), and cerebrospinal fluid (CSF) to support AD diagnosis in symptomatic individuals [4]. The use of neuroimaging techniques such as MRI and CT allows the study of neurodegenation or neuronal injury due to AD in vivo, while the analysis of CSF and PET studies allow assessing brain amyloidosis and taupathy [8]. Unfortunately, these biomarkers present several disadvantages that limit their wide clinical application, in particular in low- and middle-income countries. First, obtaining CFS samples is an invasive procedure. Second, neuroimaging tools are physically constrained, thus can be stressful for elderly patients. They are also costly to fund and require experts to operate the machines and analyse the results. These limitations are exacerbated in low- and medium-income countries, as well as in remote and rural regions in developed countries, e.g. Canada's North, thus requiring displacements that are neither comfortable nor practical for the patient. Driven by the drawbacks and limitations of CFS- and neuroimaging-derived biomarkers, electroencephalography (EEG)-based biomarkers have emerged as a promising alternative to develop easier and more convenient diagnostic solutions.

EEG consists of recording changes in time of the electrical activity in the cerebral cortex measured through electrodes placed on the individuals scalp [9]. As EEG signals reflect functional changes in the cerebral cortex, EEG biomarkers have been used to assess neuronal degeneration caused by AD, reaching diagnostic accuracy levels around 70-90%, which are in line with those obtained with other type of biomarkers. EEG, however, has the advantages of being non-invasive, potentially portable and less expensive [10]–[15]. In the EEG-based study of AD, EEG signals are typically recorded with the participants awake and without the presence of any stimulus, this condition is known as resting-state EEG (rsEEG). The utilization of rsEEG over other acquisition paradigms responds to the advantages this condition presents, such as not requiring the participant to perform a task, hence reducing the detrimental effects of movement and eye artifacts, as well as simpler acquisition setups, hence reducing costs and improving portability [15].

Regarding the number of electrodes, over 90% of published works have relied on medium- or high-density EEG devices (16+ electrodes) [15]. While a higher number of electrodes can provide richer information on the underlying brain activity, such device layouts are expensive and require long setup times, which can be stressful for elderly patients. Lower-density layouts could potentially overcome this issue, whilst improving portability and reducing costs.

Regarding classical rsEEG features used for AD diagnosis, most works have relied on the five major frequency subbands,

978-1-7281-4569-3/19/$31.00 ©2019 IEEE

namely: delta (δ) 0.1-4 Hz, theta (θ) 4-8 Hz, alpha (α) 8-12 Hz, beta (β) 12-30 Hz and gamma (γ) >30 Hz. The definition of these bands has helped to standardize experimental protocols and has provided useful insights about brain functionality and synchronization [9], [16], and has allowed for different features to be directly compared [12], [15]. However, these frequency subbands may not be the optimal for AD, as they have been defined based on visual inspection of EEG signals in healthy subjects [9]. As such, recent works have shown that other frequency bands can be optimized for AD diagnosis (e.g., [17], [18]).

In this work, we are interested in developing an AD diagnostic device that relies on a low-density EEG layout and can rely on raw rsEEG signals. Recently, we showed that amplitude modulation spectral analysis of EEG signals resulted in artifact-robust features for AD [19]. When coupled with an automated artifact removal algorithm, modulation spectral features relying on conventional frequency band decomposition resulted in reliable AD diagnostic accuracy using a layout with 20 electrodes. A recent exploration suggested that alternative frequency bands may also be beneficial for the modulation spectral features [20]. Here, we build upon these findings and explore "patches" in the amplitude modulation power spectrogram that are less sensitive to artifacts and that convey information to discriminate not only controls from AD patients, but also AD patients of varying disease severity levels.

TABLE I

PARTICIPANT DEMOGRAPHICS. GROUPS WERE AGE MATCHED BUT NOT EDUCATIONS MATCHED (NOLD VS AD1, AND NOLD VS AD2).

Group identifier	Subjects (female)	Age [years]	Education [years]	MMSE
Nold	20 (9)	68.0±8.6	10.1±5.5	28.5±1.7
AD1	19 (11)	74.1±5.5	5.6±2.8	19.4±5.3
AD2	15 (9)	75.0±11.8	4.1±3.8	12.8±5.0

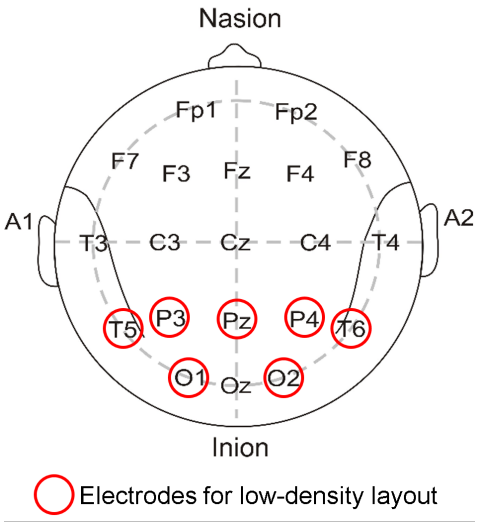

Fig. 1. EEG electrode placement.

II. METHODS AND MATERIAL

A. Participants

Fifty-four participants were recruited from the Behavioral and Cognitive Neurology Unit of the Department of Neurology and the Reference Center for Cognitive Disorders at the Hospital das Clinicas in São Paulo, Brazil. AD diagnosis was made by experienced neurologists according to NINCDS-ADRDA criteria [21] and classified based on the Brazilian version of the MMSE [22]. Participants were divided in three groups: the first group (Nold) consisted of 20 cognitively healthy normal elderly controls, the second group (AD1) comprised 19 mild-AD patients, and the third group (AD2) of 15 patients with moderate-to-severe AD symptoms. Table I presents the details in the demographic characteristics of the participants. For inclusion to the two AD groups, an additional criterion was the presence of functional and cognitive decline over the previous 12 months based on detailed interviews with knowledgeable informants. Patients from the AD groups were also screened for diabetes mellitus, kidney disease, thyroid disease, alcoholism, liver disease, lung disease or vitamin B12 deficiency, to discard other causes of cognitive decline. Ethics approval was obtained from the Research Ethics Office, as well as consent from the participants to participate in the study.

B. rsEEG acquisition and processing

During the EEG acquisition session, the participants were awake, relaxed, and with their eyes closed for at least eight minutes. Resting-state eyes-closed recording condition is the most common condition in EEG-based AD studies as it reduces artifacts due to head and eye movements, moreover, it is a comfortable and no-stressing condition suitable for elderly participants [15]. EEG signals were recorded from twenty channels with 12-bit resolution and 200 Hz sampling frequency using Braintech 3.0 instrumentation (EMSA Equipamentos Médicos INC., Brazil). The electrodes were placed according to the international 10-20 montage system, presented in Figure 1; electrode impedance was kept below 10 kΩ, and attached bi-auricular (A1 and A2) electrodes were used as reference. The recorded EEG signals were channel-wise decimated to have the 7-channel low-density layout focused on parietal and occipital lobes, as depicted in Figure 1. The selection of the electrode positions for the low-density layout were chosen based on the results presented in [20]. Moreover, based on evidence of an inter-hemispheric disconnection with AD [10], [23]–[26], three inter-hemispheric bipolar signals were also computed as the electric potential difference between pairs of electrodes in opposite hemispheres, i.e., T5-T6, P3-P4 and O1-O2. EEG recordings were filtered with a zero-phase FIR bandpass filter with a bandwidth 0.5-45 Hz.

Three different datasets were created from the acquired rsEEG signals: (*i*) signals from the entire recording without any additional processing, referred to as "raw"; (*ii*), the wavelet-enhanced independent components analysis (wICA) method was used on the raw EEG signals to automatically remove artifacts, these signals are referred to as "wICA" [27],

[28]; EEG signals in "raw" and "wICA" were divided in 8-s epochs; in the third dataset, ((*iii*), raw EEG signals were visually inspected by two experienced clinicians to obtain several 8-s artifact-free epochs; these signals are referred as "manually selected". Signal pre-processing and dataset generation was carried out with EEGLAB [29].

C. Modulation spectrum energy patches

To study the temporal changes of the spectral content of the rsEEG signals, time-frequency representations such as the short-time Fourier transform and the continuous wavelet transform (CWT) have been used with EEG [16], [30]. These representations do not provide information about the spectral periodicity, hence a second time-to-frequency transformation can be performed over the time axis of the time-frequency representation. The end result is a modulation spectral representation which depicts the second-order periodicities that would otherwise not be present with conventional spectral or time-frequency representations [31], [32].

In our experiments, the power modulation spectrogram was used. For each EEG channel, $x(t)$, the spectrotemporal representation, $X(t, f)$, was computed using the CWT with the complex Morlet wavelet for frequencies from 1 to 45 Hz with 1-Hz step and n_c = 6. From this time-frequency representation, the power modulation spectrogram was calculated as per (1), for each 8-second epoch in the rsEEG recordings. To allow for comparison among subjects, each power modulation spectrogram is normalized to unit power.

$$X(f, f_{mod}) = \mathcal{F}_t \left\{ |X(t, f)|^2 \right\}. \tag{1}$$

From the results presented in [20], three modulation power "patches," or regions of interest, stand out as resulting in the most discriminatory power between healthy controls and AD patients. By using source localization, it has been found that the active brain areas that give origin to these modulation patches are accordant with the results reported in AD literature with different neuroimaging modalities [20]. Figure 2 depicts the three patches found, which are referred to as R_1, R_2, and R_3. The power in these patches correspond to the normalized power inside the regions of interest, i.e.,:,

$$P_i = \iint_{R_i} |X(f, f_{mod})|^2 df\, df_{mod}. \tag{2}$$

Ratios between the features P_1, P_2 and P_3 were also computed, namely, P_1/P_3, P_2/P_1 and P_2/P_3. As such, a total of six new features are computed for each of the seven rsEEG signals and the three inter-hemispheric bipolar signals. We call this feature set "RG3". For benchmarking purposes, power spectral features (termed "PSD") and conventional amplitude modulation rate-of-change features ("MOD") were also computed. Both benchmark feature sets rely on traditional frequency subband decompositions. The interested reader is referred to [19] for more details about the benchmarks. Table II lists all the benchmark and proposed features explored in this study. All features were computed

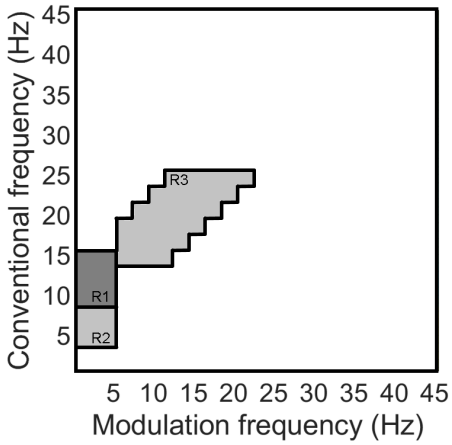

Fig. 2. Modulation spectral power patches for AD diagnosis

TABLE II
LIST OF COMPUTED FEATURES FOR EACH 8-S EPOCH.

Feature group	Features
Modulation domain features (RG3)	P_1 P_2 P_3 P_1/P_3 P_2/P_1 P_2/P_3
Spectral features (PSD)	delta theta alpha low-alpha high-alpha beta delta-beta theta-beta gamma
Amplitude modulation rate-of-change (MOD)	delta-mdelta theta-mdelta theta-mtheta alpha-mdelta alpha-mtheta beta-mdelta beta-mtheta beta-malpha beta-mbeta gamma-mdelta gamma-mtheta gamma-malpha gamma-mbeta gamma-mgamma

for each of the 10 channels (7 monopolar + 3 bipolar), in 8-seconds windows, for the manually selected, raw and wICA datasets. Diagnostic accuracy was computed for each feature set alone, as well as for the following two combinations: PSD features and MOD features ("PSD+MOD"), and PSD features and RG3 features ("PSD+RG3").

D. Feature selection and classification

For each subject, 25% of the available epochs were used to perform feature selection. The top-24 features were selected based on ANOVA F-value between feature and labels. For the classification stage, a support vector machine (SVM) classifier was used, with the following parameters: radial basis function (RBF) kernel, hyper-parameter γ = 1/24, with 24 being the number of features, and default regularization parameter of C = 1. Leave-one-subject-out cross-

TABLE III

ACCURACY FOR THE NOLD VS. AD TASK. VALUES IN BOLD INDICATE THE BEST PERFORMANCE PER DATASET.

	Feature Sets				
EEG dataset	PSD	MOD	RG3	PSD+MOD	PSD+RG3
manual	81.5	81.5	**88.9**	81.5	81.5
raw	77.8	64.8	74.1	77.8	**79.6**
wICA	72.2	61.1	72.2	**75.9**	**75.9**
manual (20 electrodes)	79.7	75.9	**88.9**	79.6	81.5

TABLE IV

ACCURACY FOR THE NOLD VS. AD1 TASK. VALUES IN BOLD INDICATE THE BEST PERFORMANCE PER DATASET.

	Feature Sets				
EEG dataset	PSD	MOD	RG3	PSD+MOD	PSD+RG3
manual	74.4	**82.1**	74.4	69.2	64.1
raw	**69.2**	56.4	**69.2**	66.7	**69.2**
wICA	64.1	56.4	56.4	61.5	**66.7**
manual (20 electrodes)	**82.1**	71.8	76.9	79.5	74.4

validation was utilized. Feature selection and classification stages were carried out with the open-source scikit-learn (machine learning for Python) package [33]. The final label predicted for each subject relied on majority vote over all epoch predictions. As figures-of-merit, diagnostic accuracy was reported subject-wise for the manually selected, raw and wICA datasets for four classification tasks: (*i*) Nold vs. AD, (*ii*) Nold vs. AD1, (*iii*) AD1 vs. AD2, and (*iv*) Nold vs AD1 vs AD2.

III. EXPERIMENTAL RESULTS AND DISCUSSION

Tables III-VI list the accuracy obtained for tasks *i*-*iv*, respectively, for the different datasets (manually selected, raw, and wICA) and feature sets (PSD, MOD, RG3, PSD+MOD, and PSD+RG3). For comparison purposes, a gold standard based on manually selected rsEEG segments and a full 20-electrode layout is also shown.

TABLE V

ACCURACY FOR THE AD1 VS. AD2 TASK. VALUES IN BOLD INDICATE THE BEST PERFORMANCE PER DATASET.

	Feature Sets				
EEG dataset	PSD	MOD	RG3	PSD+MOD	PSD+RG3
manual	**64.7**	58.8	**64.7**	61.8	**64.7**
raw	**73.5**	64.7	67.6	**73.5**	70.6
wICA	67.6	67.6	**73.5**	64.7	67.6
manual (20 electrodes)	67.6	50.0	67.6	61.8	**79.4**

TABLE VI

ACCURACY FOR THE NOLD VS. AD1 VS. AD2 TASK. VALUES IN BOLD INDICATE THE BEST PERFORMANCE PER DATASET.

	Feature Sets				
EEG dataset	PSD	MOD	RG3	PSD+MOD	PSD+RG3
manual	57.4	51.9	**64.8**	61.1	**64.8**
raw	51.9	44.4	53.7	**57.4**	44.4
wICA	**61.1**	38.9	51.9	50.0	51.9
manual (20 electrodes)	61.1	50.0	61.1	**63.0**	**63.0**

As can be seen, for the Nold vs AD task, the proposed features achieved the highest accuracy with the manually selected dataset and achieved overall accuracy inline with the gold standard. When considering only the raw signals, PSD showed the best performance of the individual feature sets, achieving an accuracy of 77.8%. When combined with the proposed RG3 feature, however, further gains were observed and an overall accuracy of 79.6% could be seen. These results are promising, as they rely on a low-density setup and do not require any artifact removal steps.

As the modulation spectral power patches used herein were motivated by Nold vs AD (AD1+AD2) discrimination insights from [20], the accuracies reported in Table III were the highest. Notwithstanding, comparison of the proposed features against the benchmarks for the three other tasks will allow us to better understand the potential of the proposed features, in particular their robustness against artifacts.

For the Nold vs AD1 task, the proposed feature set achieved the best accuracy for the raw dataset, alongside the PSD features. In this case, feature fusion did not improve accuracy and resulted in an overall accuracy of 69.2%. These results are encouraging and suggest that very early detection may be possible, though some improvements are still needed. When exploring the effects of varying levels of AD, conventional PSD and PSD+MOD features resulted in the best accuracy, suggesting that the selected power patches are not optimal for severity level tracking. Interestingly, for the majority of the classification tasks, the performance of features from "raw" dataset is better than the one obtained with features from the"wICA" dataset; this may have its origin in the effects of the automated processing of EEG, as it may remove relevant discriminatory information from raw EEG data [28], this requires further exploration. Lastly, when performing 3-class discrimination, the proposed features showed optimal only for the manually selected case. Lastly, when comparing the results from the gold standard to the proposed low-density solution, it is clear that a performance drop exists, though the advantage of not requiring any human intervention for segment selection and faster preparation time can outweigh the lower accuracy achieved.

IV. CONCLUSION

When studying Alzheimer's disease, low-density portable EEG devices present interesting advantages compared to medium- and high-density research counterparts. Representative examples include (*i*) reduced hardware-related stress during EEG setup, thus reduced discomfort during recordings, allowing longer recordings in more natural positions or circumstances, (*ii*) since wiring is drastically reduced, transportation of these devices is improved, and (*iii*) low-density devices present practical benefits in clinical practice by reducing the setup time and stress related to the use of EEG devices on elderly participants. In this paper, we explored the first steps towards developing a diagnostic system based on low-density devices and raw rsEEG inputs. New modulation spectral power patches are proposed as features and we show that a system relying on seven electrodes and

raw inputs can achieve control vs AD discrimination at the same level as a gold standard method based on 20 electrodes and manually-selected EEG segments. Alternative patches are needed in order to extract feature optimized for alternate disease monitoring tasks, such as disease level progression.

REFERENCES

[1] M. Prince, A. Wimo, M. Guerchet, G.-C. Ali, Y.-T. Wu, and M. Prina, "World Alzheimer Report 2015, The Global Impact of Dementia: An analysis of prevalence, incidence, cost and trends," *Alzheimer's Disease International*, p. 87, 2015.

[2] C. Patterson, "World Alzheimer Report 2018: The State of the Art of Dementia Research: New Frontiers," *Alzheimer's Disease International (ADI): London, UK*, 2018.

[3] D. Galimberti and E. Scarpini, "Disease-modifying treatments for Alzheimer's disease," *Therapeutic Advances in Neurological Disorders*, vol. 4, no. 4, pp. 203–216, Jul. 2011, 00037.

[4] C. R. Jack *et al.*, "Introduction to the recommendations from the National Institute on Aging-Alzheimer's Association workgroups on diagnostic guidelines for Alzheimer's disease," *Alzheimer's & Dementia: The Journal of the Alzheimer's Association*, vol. 7, no. 3, pp. 257–262, May 2011.

[5] G. M. McKhann *et al.*, "The diagnosis of dementia due to Alzheimer's disease: Recommendations from the National Institute on Aging-Alzheimer's Association workgroups on diagnostic guidelines for Alzheimer's disease," *Alzheimer's & Dementia: The Journal of the Alzheimer's Association*, vol. 7, no. 3, pp. 263–269, May 2011.

[6] M. S. Albert *et al.*, "The diagnosis of mild cognitive impairment due to Alzheimer's disease: Recommendations from the National Institute on Aging-Alzheimer's Association workgroups on diagnostic guidelines for Alzheimer's disease," *Alzheimer's & Dementia: The Journal of the Alzheimer's Association*, vol. 7, no. 3, pp. 270–279, May 2011.

[7] R. A. Sperling *et al.*, "Toward defining the preclinical stages of Alzheimer's disease: Recommendations from the National Institute on Aging-Alzheimer's Association workgroups on diagnostic guidelines for Alzheimer's disease," *Alzheimer's & Dementia: The Journal of the Alzheimer's Association*, vol. 7, no. 3, pp. 280–292, May 2011.

[8] C. R. Jack *et al.*, "NIA-AA Research Framework: Toward a biological definition of Alzheimer's disease," *Alzheimer's & Dementia*, vol. 14, no. 4, pp. 535–562, Apr. 2018.

[9] P. L. Nunez and R. Srinivasan, *Electric Fields of the Brain: The Neurophysics of EEG*. Oxford; New York: Oxford University Press, 2006, 03143.

[10] J. Jeong, "EEG dynamics in patients with Alzheimer's disease," *Clinical Neurophysiology*, vol. 115, no. 7, pp. 1490–1505, Jul. 2004, 00543.

[11] J. Dauwels, F. Vialatte, and A. Cichocki, "Diagnosis of Alzheimer's Disease from EEG Signals: Where Are We Standing?" *Current Alzheimer Research*, vol. 7, no. 6, pp. 487–505, Sep. 2010, 00108.

[12] R. Lizio, F. Vecchio, G. B. Frisoni, R. Ferri, G. Rodriguez, and C. Babiloni, "Electroencephalographic Rhythms in Alzheimer's Disease," *International Journal of Alzheimer's Disease*, vol. 2011, pp. 1–11, 2011.

[13] G. G. Yener and E. Basar, "Biomarkers in Alzheimer's disease with a special emphasis on event-related oscillatory responses," *Suppl. Clin. Neurophysiol*, vol. 62, pp. 237–273, 2013.

[14] A. Alberdi, A. Aztiria, and A. Basarab, "On the early diagnosis of Alzheimer's Disease from multimodal signals: A survey," *Artificial Intelligence in Medicine*, vol. 71, pp. 1–29, Jul. 2016.

[15] R. Cassani, M. Estarellas, R. San-Martin, F. J. Fraga, and T. H. Falk, "Systematic Review on Resting-State EEG for Alzheimer's Disease Diagnosis and Progression Assessment," *Disease Markers*, vol. 2018, 2018.

[16] L. Sörnmo and P. Laguna, *Bioelectrical Signal Processing in Cardiac and Neurological Applications*. Academic Press, 2005, vol. 8.

[17] M. Elgendi, F. Vialatte, A. Cichocki, C. Latchoumane, Jaesung Jeong, and J. Dauwels, "Optimization of EEG frequency bands for improved diagnosis of Alzheimer disease." IEEE, Aug. 2011, pp. 6087–6091.

[18] E. Gallego-Jutglà, J. Solé-Casals, F.-B. Vialatte, M. Elgendi, A. Cichocki, and J. Dauwels, "A hybrid feature selection approach for the early diagnosis of Alzheimer's disease," *Journal of Neural Engineering*, vol. 12, no. 1, p. 016018, Feb. 2015.

[19] R. Cassani, T. H. Falk, F. J. Fraga, M. Cecchi, D. K. Moore, and R. Anghinah, "Towards automated electroencephalography-based Alzheimer's disease diagnosis using portable low-density devices," *Biomedical Signal Processing and Control*, vol. 33, pp. 261–271, Mar. 2017.

[20] R. Cassani and T. H. Falk, "Alzheimer's disease diagnosis and severity progression monitoring based on new electroencephalography modulation spectral features," *Journal of Biomedical and Health Informatics (Submitted)*, 2019.

[21] G. McKhann, D. Drachman, M. Folstein, R. Katzman, D. Price, and E. Stadlan, "Clinical diagnosis of alzheimer's disease: Report of the NINCDS-ADRDA work group⋆ under the auspices of department of health and human services task force on alzheimer's disease," *Neurology*, vol. 34, no. 7, pp. 939–944, 1984, cited By 21876.

[22] S. Brucki, R. Nitrini, P. Caramelli, P. H. Bertolucci, and I. H. Okamoto, "Suggestions for utilization of the mini-mental state examination in Brazil," *Arquivos de neuro-psiquiatria*, vol. 61, no. 3B, pp. 777–781, 2003.

[23] F. J. Fraga *et al.*, "Towards an EEG-based biomarker for Alzheimer's disease: Improving amplitude modulation analysis features," in *2013 IEEE International Conference on Acoustics, Speech and Signal Processing (ICASSP)*, May 2013, pp. 1207–1211.

[24] T. H. Falk, F. J. Fraga, L. Trambaiolli, and R. Anghinah, "EEG amplitude modulation analysis for semi-automated diagnosis of Alzheimer's disease," *EURASIP Journal on Advances in Signal Processing*, vol. 2012, no. 1, pp. 1–9, 2012, 00012.

[25] L. R. Trambaiolli, A. C. Lorena, F. J. Fraga, P. A. M. K. Kanda, R. Nitrini, and R. Anghinah, "Does EEG Montage Influence Alzheimer's Disease Electroclinic Diagnosis?" *International Journal of Alzheimer's Disease*, vol. 2011, pp. 1–6, 2011.

[26] L. R. Trambaiolli, A. C. Lorena, F. J. Fraga, P. A. Kanda, R. Anghinah, and R. Nitrini, "Improving Alzheimer's Disease Diagnosis with Machine Learning Techniques," *Clinical EEG and Neuroscience*, vol. 42, no. 3, pp. 160–165, Jul. 2011.

[27] N. P. Castellanos and V. A. Makarov, "Recovering EEG brain signals: Artifact suppression with wavelet enhanced independent component analysis," *Journal of Neuroscience Methods*, vol. 158, no. 2, pp. 300–312, Dec. 2006, 00126.

[28] R. Cassani, T. H. Falk, F. J. Fraga, P. A. M. Kanda, and R. Anghinah, "The effects of automated artifact removal algorithms on electroencephalography-based Alzheimer's disease diagnosis," *Frontiers in Aging Neuroscience*, vol. 6, p. 55, 2014, 00002.

[29] A. Delorme and S. Makeig, "EEGLAB: An open source toolbox for analysis of single-trial EEG dynamics including independent component analysis," *Journal of neuroscience methods*, vol. 134, no. 1, pp. 9–21, 2004, 04104.

[30] M. Cohen, *Analyzing Neural Time Series Data: Theory and Practice*. MIT Press, 2014.

[31] L. Atlas and S. A. Shamma, "Joint acoustic and modulation frequency," *EURASIP Journal on Advances in Signal Processing*, vol. 2003, no. 7, p. 310290, 2003.

[32] R. Cassani and T. H. Falk, "Spectrotemporal Modeling of Biomedical Signals: Theoretical Foundation and Applications," in *Reference Module in Biomedical Sciences*. Elsevier, 2018.

[33] F. Pedregosa *et al.*, "Scikit-learn: Machine Learning in Python," *J. Mach. Learn. Res.*, vol. 12, pp. 2825–2830, Nov. 2011.